

THE MOST LUMINOUS SUPERNOVAE

TUGULDUR SUKHBOLD¹ AND S. E. WOOSLEY¹(Accepted —, 2016)
15 Feb, 2016

ABSTRACT

Recent observations have revealed an amazing diversity of extremely luminous supernovae, seemingly increasing in radiant energy without bound. We consider here the physical limits of what existing models can provide for the peak luminosity and total radiated energy for non-relativistic, isotropic stellar explosions. The brightest possible supernova is a Type I explosion powered by a sub-millisecond magnetar. Such models can reach a peak luminosity of 2×10^{46} erg s⁻¹ and radiate a total energy of 4×10^{52} erg. Other less luminous models are also explored, including prompt hyper-energetic explosions in red supergiants, pulsational-pair instability supernovae, and pair-instability supernovae. Approximate analytic expressions and limits are given for each case. Excluding magnetars, the peak luminosity is near 1×10^{44} erg s⁻¹ for the brightest models. The corresponding limits on total radiated power are 3×10^{51} erg (Type I) and 1×10^{51} erg (Type II). A magnetar-based model for the recent transient event, ASASSN-15lh is presented that strains, but does not exceed the limits of what the model can provide.

Subject headings: stars: supernovae: general

1. INTRODUCTION

Motivated by the recent discovery of many ultraluminous supernovae (ULSNe), including, possibly, the extreme case of ASASSN-15lh (Dong et al. 2016), the limits of several scenarios often invoked for their interpretation are considered. These include prompt, point-like central explosions with very high energy, colliding shells, pair-instability supernovae, and newly-born magnetars (e.g. Gal-Yam 2012; Quimby et al. 2011). Each of these energy sources will give different results when occurring in a stripped core of helium or carbon and oxygen (Type I) or a red supergiant (Type II) and both cases are considered. All calculations of explosions and light curves use the 1D implicit hydrodynamics code KEPLER (Weaver et al. 1978; Woosley et al. 2002), and employ presupernova models that have already been published.

The even more extreme case of “relativistic supernovae” - either supernovae with relativistic jets or the explosion of super-massive stars that collapse because of general relativistic instability (Fuller et al. 1986; Chen et al. 2014) is not considered here. These are rare events with their own distinguishing characteristics.

2. PROMPT EXPLOSIONS AND PAIR-INSTABILITY

Any explosive energy that is deposited before the ejecta significantly expands will suffer severe adiabatic degradation that will prevent the supernova from being particularly bright. An upper bound for prompt energy deposition in a purely neutrino-powered explosion is $\sim 3 \times 10^{51}$ erg (Fryer & Kalogera 2001; Ugliano et al. 2012), which is capable of explaining common supernovae (Woosley et al. 2007), but not the more luminous ones. In a red, or worse, blue supergiant, the expansion from an initial stellar radius of, at most, 10^{14} cm, to a few times 10^{15} cm, where recombination occurs, degrades the total electromagnetic energy available to $\lesssim 10^{50}$ erg. Even

in the most extreme hypothetical case, where a substantial fraction of a neutron star binding energy, $\sim 10^{53}$ erg deposits instantly, the light curve is limited to a peak brightness of approximately 10^{44} erg s⁻¹ (neglecting the very brief phase of shock break out).

This can be demonstrated analytically and numerically. Adopting the expression for plateau luminosity and duration from Popov (1993) and Kasen & Woosley (2009), as calibrated to numerical models by Sukhbold et al. (2015), Type II supernovae have a luminosity on their plateaus of

$$L_p = 8.5 \times 10^{43} R_{0,500}^{2/3} M_{env,10}^{-1/2} E_{53}^{5/6} \text{ erg s}^{-1}, \quad (1)$$

where $R_{0,500}$ is the progenitor radius in $500 R_\odot$, $M_{env,10}$, the envelope mass in $10 M_\odot$, and E_{53} , the prompt explosion energy in units of 10^{53} erg. The approximate duration of the plateau, ignoring the effects of radioactivity, is given by

$$\tau_p = 41 E_{53}^{-1/6} M_{10}^{1/2} R_{0,500}^{1/6} \text{ days}. \quad (2)$$

This plateau duration is significantly shorter than common supernovae due to the much higher energies considered.

These relations compare favorably with a model for a $15 M_\odot$ explosion calculated with an assumed explosion energy of 0.5×10^{53} erg (Fig. 1). Here the red supergiant presupernova stellar model from Sukhbold & Woosley (2014) had a radius of $830 R_\odot$ and an envelope mass, $8.5 M_\odot$. The estimated luminosity on the plateau from eq. (1) is 6.7×10^{43} erg s⁻¹ and duration from eq. (2) is 46 days. The corresponding KEPLER model in Fig. 1 had a duration of ~ 45 days and a luminosity at day 25 of 6.6×10^{43} erg s⁻¹. The total energy emitted is approximately $L_p \tau_p$, or $3 \times 10^{50} E_{53}^{2/3} R_{0,500}^{5/6}$ erg.

Similar limits characterize a pair-instability supernova (PSN) in a red supergiant progenitor. Again, maximum explosion energies are $\lesssim 10^{53}$ erg (Heger & Woosley 2002).

¹ Department of Astronomy and Astrophysics, University of California, Santa Cruz, CA 95064. sukhbold@ucolick.org

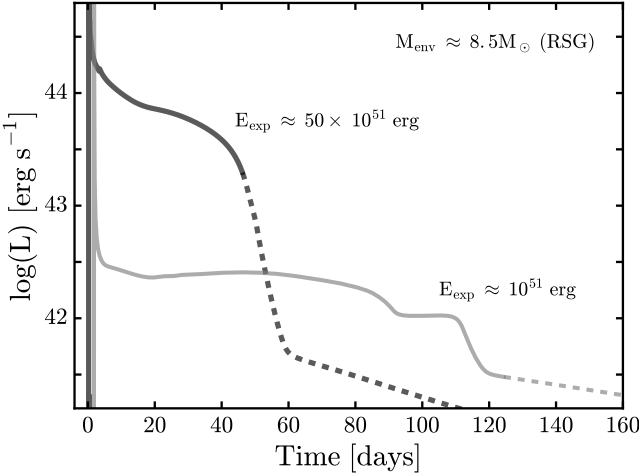


FIG. 1.— Bolometric light curves for a $15 M_{\odot}$ supergiant exploded with two different values of prompt energy deposition. One, 10^{51} erg, is typical of common Type IIP supernovae; the other, 50×10^{51} erg is near the upper bound of what any prompt, point explosion might provide. Even for this extreme case, the plateau luminosity does not exceed $\sim 10^{44}$ erg s $^{-1}$. The curves are dashed when the ejecta become optically thin and the blackbody representation of their emission becomes questionable. The presupernova star, originally $15 M_{\odot}$ at birth, had a mass of $12.6 M_{\odot}$, of which $8.5 M_{\odot}$ was hydrogen envelope, and a radius of $R_{0,500} \sim 1.7$. The luminosity at break out in the more energetic model peaked at 1.5×10^{47} erg s $^{-1}$, but only lasted for about 100 seconds.

For the most extreme, rarest case, $M_{10} \approx 20$, $R_{0,500} \approx 5$ and $E_{53} \approx 1$, eq. (1) and eq. (2) imply plateau luminosities near 5×10^{43} erg s $^{-1}$ for about 200 days. These values are consistent with KEPLER models given in Scannapieco et al. (2005). The total radiated energy is 1×10^{51} erg. Most of the radioactivity decays during the plateau and, since its energy is substantially less than the explosion energy, the modification of the light curve during its bright plateau is not appreciable.

A PSN can be brighter for a shorter period of time if it has lost its envelope and makes a lot of ^{56}Ni . The rarest, most massive PSN produces, at most, $50 M_{\odot}$ of ^{56}Ni in an explosion with final kinetic energy of 9×10^{52} erg (Heger & Woosley 2002). This large production only occurs for the the most massive helium cores ($\sim 130 M_{\odot}$), which very nearly collapse to black holes. The total energy available from the decay of large amount of ^{56}Ni is substantial,

$$E_{\text{dec}} \approx 2.4 \times 10^{51} \left(\frac{M_{\text{Ni}}}{50 M_{\odot}} \right) (3e^{-t/\tau_{\text{Co}}} + e^{-t/\tau_{\text{Ni}}}) \text{ erg}, \quad (3)$$

here M_{Ni} is the ^{56}Ni mass in M_{\odot} , $\tau_{\text{Co}} = 111$ and $\tau_{\text{Ni}} = 8.7$ are mean lives of ^{56}Co and ^{56}Ni in days. For a nickel mass of $\sim 50 M_{\odot}$ the total energy is nearly 10^{52} erg. Most of this energy is lost during the adiabatic expansion to peak, however.

An approximate estimate when the PSN light curve peaks is given by equating the effective diffusion timescale, t_d , to age. This gives a time of peak luminosity, t_p , of

$$t_p = \left(\frac{3\kappa}{4\pi c} \right)^{1/2} \left(\frac{M_{\text{ej}}^3}{2E_{\text{exp}}} \right)^{1/4} \quad (4)$$

$$t_p \sim 177 \left(\frac{M_{\text{ej}}}{130 M_{\odot}} \right)^{3/4} \left(\frac{E_{\text{exp}}}{10^{53} \text{ erg}} \right)^{-1/4} \text{ days},$$

where M_{ej} is the ejecta mass in M_{\odot} and E_{exp} is the explosion energy in erg. Considering the similarity of high velocity and iron-rich composition to Type Ia supernovae, an opacity, $\kappa \approx 0.1 \text{ cm}^2 \text{ g}^{-1}$ is assumed. Arnett's Rule (Arnett 1979) then implies a maximum luminosity of

$$L_p \approx 8 \times 10^{44} \left(\frac{M_{\text{Ni}}}{50 M_{\odot}} \right) e^{-t_p/\tau_{\text{Co}}} \text{ erg s}^{-1}. \quad (5)$$

Only the luminosity due to the decay of ^{56}Co is included here, since for $t \sim t_p$, most of ^{56}Ni will have already decayed. For the fiducial values of t_p and M_{Ni} , the peak luminosity is roughly 1.5×10^{44} erg s $^{-1}$, which compares favourably with models in which the hydrodynamics and radiation transport are treated carefully (Kasen et al. 2011; Kozyreva & Blinnikov 2015).

Assuming that the total emitted energy for a Type I supernova as

$$E_{\text{rad}} \approx \frac{1}{2} L_p t_p + E_{\text{dec}}(t_p), \quad (6)$$

and using the fiducial values, the approximate upper bound on the total luminous energy in a PSN-Type I is 2.6×10^{51} erg, about one quarter of the total decay energy.

3. THE COLLISION OF SHELLS

The luminosity of colliding shells is limited by their differential kinetic energy, their masses, and the radii at which they collide. If the collision happens at too small a radius where the ejecta is still very optically thick, colliding shells become another variant of “prompt explosions” (§ 2). Most of the collision energy is adiabatically degraded. On the other hand, if the collision happens at too large a radius, the resulting transient has a longer time scale, lower luminosity, and may not even emit chiefly in the optical. In practice, these constraints limit the radius where the shells collide and produce a bright optical transient to roughly $10^{15} - 10^{16}$ cm. A similar range of radii is obtained by multiplying typical collision speeds, 1000 to 4000 km s $^{-1}$, by the duration of an ULSN, $\sim 100 - 200$ days.

Models based upon colliding shells can, in principle, be extremely luminous. A red supergiant that ejected its envelope at 1000 km s^{-1} a year before dying, and then exploded in a final blast of 10^{53} erg could produce an optical event approaching 10^{46} erg s $^{-1}$ for 100 days. The physics powering such an event is entirely missing, however. More plausible models eject less mass (Shiode & Quataert 2014), or have much lower explosion energy (Woosley & Heger 2015a). These models might provide a few times 10^{50} erg spread over 100 days (Woosley & Heger 2015a, e.g.), but much more than that would require a very energetic core explosion that has not been demonstrated.

The most luminous colliding shell models in the published literature are pulsational-pair instability supernovae (PPSN; Woosley et al. 2007; Yoshida et al. 2016). For a narrow range of masses corresponding to stars with $50 - 55 M_{\odot}$ helium cores, a supergiant star, red or blue, will eject its hydrogen envelope at speeds $\sim 1000 \text{ km s}^{-1}$, and a year or so later eject one or more very energetic shells that would smash into it (Woosley & Heger 2015b). The source of the energy is the thermonuclear burning of

carbon and oxygen. For lighter helium cores, low energy shells are ejected in rapid succession before the envelope has expanded to 10^{15} cm. The collision energy is adiabatically degraded and the resulting supernova is not especially luminous (Woosley 2016, in prep.). For heavier cores, the pulses are too far in between to produce collisions inside of 10^{16} cm that last only a hundred days or so. The resulting outbursts are too long and faint, and may not even lie in the optical band.

In the narrow helium-core mass range of $50 - 55 M_{\odot}$ though, one or more pulses, after the one that ejects the envelope, eject additional shells carrying a power of up to 1×10^{51} erg (Woosley & Heger 2015b). Radiating all this energy over a 10^7 s interval gives a luminosity that can approach 10^{44} erg s $^{-1}$, though usually the energy is shared among several pulses, the optical conversion is not 100%, and the light curve is substantially fainter (Woosley et al. 2007).

For helium cores lacking any hydrogen envelope the luminosities are less because of the lack of a massive low velocity reservoir to turn kinetic energy into light. Typical peak luminosities for Type I supernovae are thus near 3×10^{43} erg s $^{-1}$, and the light curve can be more highly structured (Woosley & Heger 2015b).

In summary, the total radiated energy from colliding shells in the absence of a very energetic core explosion yet to be demonstrated, is unlikely to be greater than 10^{51} erg and the luminosities will be no more than 10^{44} erg s $^{-1}$.

4. MAGNETARS

With some tuning, the energy deposited by a young magnetar in the ejecta of a supernova can very significantly brighten its light curve. The idea that magnetars might underlie the production of a broad class of ULSNe has been promoted by Woosley (2010) and Kasen & Bildsten (2010) following an earlier suggestion by Maeda et al. (2007), and has been successfully applied to numerous observations of mostly ULSNe-Type I (e.g. Inserra et al. 2013; Nicholl et al. 2013; Howell et al. 2013)

The rotational kinetic energy of a magnetar with a period $P_{\text{ms}} = P/\text{ms}$ is approximately $E_{\text{m}} \approx 2 \times 10^{52} P_{\text{ms}}^{-2}$ erg. Here, $E_{\text{m},\text{max}} \approx 4 \times 10^{52}$ erg is the rotational energy for an initial period of ~ 0.7 ms. As Metzger et al. (2015) have recently discussed, the limiting rotational kinetic energy before gravitational radiation causes rapid damping might even exceed 10^{53} erg, depending on the neutron star mass and the equation of state. This energy reservoir can be tapped through vacuum dipole emission, which is approximately $E_{\text{m}}/t_{\text{m}} \approx 10^{49} B_{15}^2 P_{\text{ms}}^{-4}$ erg s $^{-1}$, where $B_{15} = B/10^{15}$ G is the dipole field strength at the equator, and $t_{\text{m}} = 2 \times 10^3 P_{\text{ms}}^2 B_{15}^{-2}$ s is the magnetar spin-down timescale. A magnetic dipole moment $B(10\text{km})^3$ is adopted, and an angle of $\pi/6$ between the magnetic and rotational axes has been assumed. Combining these relations, one obtains the temporal evolution of the rotational energy and magnetar luminosity as $E_{\text{m}}(t) = E_{\text{m},0} t_{\text{m}}/(t_{\text{m}} + t)$ and $L_{\text{m}}(t) = E_{\text{m},0} t_{\text{m}}/(t_{\text{m}} + t)^2$.

Following Kasen & Bildsten (2010), a peak luminosity can be estimated using the diffusion equation and by ignoring the radiative losses in the first law of thermo-

dynamics:

$$L_{\text{p}} = \frac{E_{\text{m},0}}{t_{\text{d}}} \left[\xi \ln \left(1 + \frac{1}{\xi} \right) - \frac{\xi}{1 + \xi} \right], \quad (7)$$

where $\xi = t_{\text{m}}/t_{\text{d}}$ is the ratio of spin-down to effective diffusion timescales. The term inside square brackets has a maximum at $\xi \approx 1/2$, obtained by solving $d(L_{\text{p}} t_{\text{d}}/E_{\text{m},0})/d\xi = 0$. This implies an optimal field strength for maximizing the peak luminosity is:

$$B_{15} \Big|_{L_{\text{p},\text{max}}} \simeq 66 P_{\text{ms},0} t_{\text{d}}^{-1/2}. \quad (8)$$

That is, for a given combination of $P_{\text{ms},0}$ and ejecta parameters - M_{ej} , E_{sn} , κ , the brightest possible peak luminosity is obtained for this field strength.

The maximum peak luminosity is then $L_{\text{p},\text{max}} \simeq E_{\text{m}}/10t_{\text{p}}$. For the limiting initial spin of $P_{\text{ms},0} = 0.7$ ms along with $\kappa = 0.01 \text{ cm}^2 \text{ g}^{-1}$, $M_{\text{ej}} = 3.5 M_{\odot}$ and $E_{\text{sn}} = 10^{51}$ erg, the corresponding field strength is $B = 7 \times 10^{13}$ G (for $\xi = 1/2$), and the limiting peak luminosity is $L_{\text{p},\text{max}} \approx 2 \times 10^{46}$ erg s $^{-1}$. Here $E_{\text{m}} \gg E_{\text{sn}}$, therefore unless one invokes even lower κ , M_{ej} and much larger E_{m} , any transient with brighter observed luminosity will be hard to explain by the magnetar model.

Using a generalized form of Arnett's Rule (Inserra et al. 2013, e.g.), $L_{\text{m}}(t_{\text{p}}) = L_{\text{p}}$, the time for L_{p} is $t_{\text{p}} = (E_{\text{m}} t_{\text{m}} L_{\text{p}}^{-1})^{1/2} - t_{\text{m}}$. For the maximal luminosity, the corresponding peak time is then $t_{\text{p},\text{max}} \simeq 2.2t_{\text{m}}$. This can be used to estimate the limiting radiated energy in the same way as in eq. (6):

$$E_{\text{rad},\text{max}} \simeq 0.4 E_{\text{m},0}. \quad (9)$$

Any observation of total radiated energy, $E_{\text{rad}} > 4 \times 10^{52}$ erg will be hard to explain by the magnetar model.

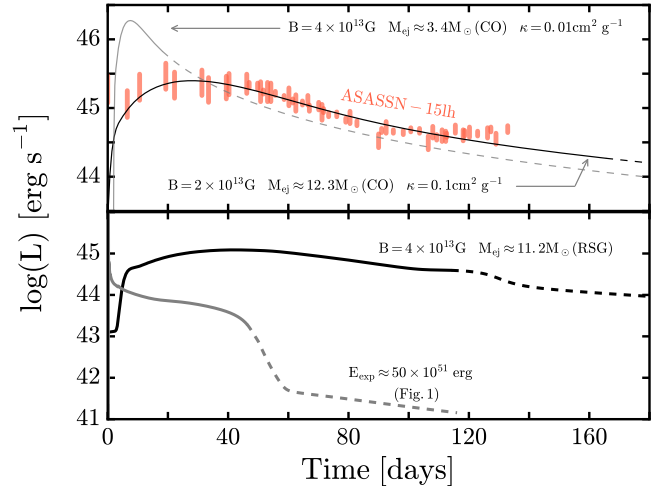


FIG. 2.— Top: The luminous transient ASASSN-15lh compared with a magnetar model. Similar magnetars embedded in less ejecta with lower opacity can, in principle, give even brighter light curves. Bottom: The same magnetar used in the top panel for fitting ASASSN-15lh is embedded in the ejecta of a massive red supergiant progenitor. The light curve is dimmer than the Type I case, but substantially brighter than the prompt explosion case shown in Fig. 1. The dashed curve marks the transition to nebular phase.

To illustrate these limits, a series of magnetar-powered

TABLE 1
LIMITING PEAK LUMINOSITIES AND RADIATED ENERGIES

	model	L_p [erg s $^{-1}$]	E_{rad} [erg]
Type II	prompt	1×10^{44}	3×10^{50}
	PSN	5×10^{43}	1×10^{51}
	PPSN	1×10^{44}	1×10^{51}
	magnetar	1×10^{45}	9×10^{51}
Type I	PSN	2×10^{44}	3×10^{51}
	PPSN	3×10^{43}	1×10^{51}
	magnetar	2×10^{46}	4×10^{52}

models based upon exploding CO cores (from Sukhbold & Woosley 2014) was calculated to find a best fit to the light curve of ASASSN-15lh. In each case, soon after bounce, the magnetar deposits its energy into the inner part of the ejecta at a rate given by the vacuum dipole spin-down. The top panel of Fig. 2 shows the best fitting model, which employs a magnetar with an initial period of 0.7 ms and magnetic field strength of 2×10^{13} G, illuminating the ejecta in the explosion of a $14 M_{\odot}$ CO core ($M_{\text{ej}} \approx 11.2 M_{\odot}$).

These magnetar parameters agree well with the previously published fits, but the ejecta masses are different. An ejecta mass of $15 M_{\odot}$ was obtained by Dai et al. (2016), as they used simple semi-analytical models, which ignored all dynamical effects and deviate from hydrodynamic calculations most when $E_m \gg E_{\text{sn}}$. An ejecta mass of only $3 M_{\odot}$ was used in Metzger et al. (2015), as they applied the same simple semi-analytical model on the early release of the data spanning only ~ 60 days. That fit would not work for the later data shown in Fig. 2, and the ejecta would become optically thin at an early time. Bersten et al. (2016) limited their models to small He-cores ($8 M_{\odot}$), and their model doesn't fit the broad peak of ASASSN-15lh well.

Also shown in the top panel is the light curve from the limiting case of a magnetar with $P_{\text{ms}} = 0.7$, $B = 2 \times 10^{13}$ G powering only $3.5 M_{\odot}$ ejecta (from $5 M_{\odot}$ CO core) with $\kappa = 0.01 \text{ cm}^2 \text{ g}^{-1}$. This model reaches $\sim 2 \times 10^{46}$ erg s $^{-1}$, however, notice that the peak is much narrower and that it becomes optically thin within just 3 weeks.

Magnetars can also illuminate bright, long lasting Type II supernovae. The bottom panel of Fig. 2, shows the same magnetar that was applied for the fit to ASASSN-15lh, now embedded inside a remnant from $15 M_{\odot}$ red supergiant progenitor. Because the ejecta mass is much larger, the light curve is fainter and much broader. The ejecta stays optically thick for nearly 4 months. Much like the radioactive decay extends the plateau duration by causing ionization, magnetar-deposited energy also significantly extends the optically thick period.

5. CONCLUSIONS

Table 1 summarizes the maximum luminosity and total luminous energy for the models considered. Given the various approximations made, the numbers are probably accurate to a factor of two in most cases. In all but the magnetar powered models, the peak luminosities are near 10^{44} erg s $^{-1}$ and peak integrated powers are near 10^{51} erg. This is gratifying since most “superluminous supernovae” are within those bounds (e.g. Nicholl et al.

2015)

For point-like explosions, which includes PSN of Type II, the prompt energy injection is typically degraded by a factor of ~ 100 by adiabatic expansion, so even obtaining 10^{51} erg requires an explosion that strains the limits of both neutron star binding energy (core-collapse supernovae) and thermonuclear energy (PSN). Given the energy input, the numbers in Table 1 rely only upon following simple radiative diffusion and recombination in a well-defined presupernova star. The results, which agree well with analytic approximations, should be quite reliable.

Similarly the upper bound for PSN-Type I is also well determined. Lacking extreme differential rotation, which would be difficult to maintain in the face of shear and magnetic torques, the dynamics of the central regions that experience the instability are not greatly influenced by rotation. One-dimensional models should suffice and unambiguously give an upper bound on the mass of ^{56}Ni made and the explosion energy (Heger & Woosley 2002). Again, model results and analytic expressions agree in predicting the luminosity and duration of the brightest possible event.

For supernovae whose light comes from colliding shells, the constraints are less accurate due to lack of knowledge about the masses, energies, and radii of the shells involved. The brightest published models are for PPSN, and there the mass of the helium core needed to make luminous optical supernovae is highly constrained. In order that the duration of the pulses be years and not months or centuries, the helium core mass needed to be in the range $50 - 55 M_{\odot}$ (slightly larger for supergiants than bare helium cores). This restricts the total energy in pulses - after the first one which ejects the envelope - to be less than 10^{51} erg. Spreading this over the necessary time scale of a year or so gives an upper bound to the luminosity, which is consistent with what has been found in detailed models thus far.

Magnetars are a special case. In principle, the most powerful source of energy is rotation. Gravitational collapse can give more, but concentrates its energy in an inefficient form - neutrinos. Radioactivity is restricted by the inefficiency of weak decay. Collisions can only utilize differential kinetic energy and must eject mass more than once. Rotation though can tap an energy reservoir almost as great as the binding energy of the neutron star and deposit it over an arbitrarily long time scale - depending on the choice of magnetic field strength. Thus the optical efficiency for converting rotational energy to light can be (forced to be) very high.

It is interesting that the upper bounds for magnetar-powered light curves are so high - greater by one to two orders of magnitude than the other models. This implies a possible observable diagnostic. Supernovae that substantially exceed 10^{44} erg s $^{-1}$ for an extended period and which have total luminous powers far above 10^{51} erg must be considered strong candidates for containing an embedded magnetar. Similarly, “supernovae” that exceed the generous limits for magnetar power given in Table 1 may not be supernovae at all.

ASASSN15-lh (Dong et al. 2016) is an interesting case in this regard. Fig. 2 shows that it can, barely, be accommodated by a magnetar model and Table 1 says it must be a magnetar, if it is a supernova (Brown 2015).

6. ACKNOWLEDGEMENTS

We thank Alex Heger for his contributions in developing the KEPLER code. This work was supported by NASA (NNX14AH34G).

REFERENCES

Arnett, W. D. 1979, *ApJ*, 230, L37

Bersten, M. C., Benvenuto, O. G., Orellana, M., & Nomoto, K. 2016, arXiv:1601.01021

Brown, P. J. 2015, The Astronomer's Telegram, 8086

Chen, K.-J., Heger, A., Woosley, S., et al. 2014c, *ApJ*, 790, 162

Dai, Z. G., Wang, S. Q., Wang, J. S., Wang, L. J., & Yu, Y. W. 2016, *ApJ*, 817, 132

Dong, S., Shappee, B. J., Prieto, J. L., et al. 2016, *Science*, 351, 257

Fryer, C. L., & Kalogera, V. 2001, *ApJ*, 554, 548

Fuller, G. M., Woosley, S. E., & Weaver, T. A. 1986, *ApJ*, 307, 675

Gal-Yam, A. 2012, *Science*, 337, 927

Heger, A., & Woosley, S. E. 2002, *ApJ*, 567, 532

Howell, D. A., Kasen, D., Lidman, C., et al. 2013, *ApJ*, 779, 98

Inserra, C., Smartt, S. J., Jerkstrand, A., et al. 2013, *ApJ*, 770, 128

Kasen, D., & Woosley, S. E. 2009, *ApJ*, 703, 2205

Kasen, D., & Bildsten, L. 2010, *ApJ*, 717, 245

Kasen, D., Woosley, S. E., & Heger, A. 2011, *ApJ*, 734, 102

Kozyreva, A., & Blinnikov, S. 2015, *MNRAS*, 454, 4357

Maeda, K., Tanaka, M., Nomoto, K., et al. 2007, *ApJ*, 666, 1069

Metzger, B. D., Margalit, B., Kasen, D., & Quataert, E. 2015, *MNRAS*, 454, 3311

Nicholl, M., Smartt, S. J., Jerkstrand, A., et al. 2013, *Nature*, 502, 346

Nicholl, M., Smartt, S. J., Jerkstrand, A., et al. 2015, *MNRAS*, 452, 3869

Popov, D. V. 1993, *ApJ*, 414, 712

Quimby, R. M., Kulkarni, S. R., Kasliwal, M. M., et al. 2011, *Nature*, 474, 487

Scannapieco, E., Madau, P., Woosley, S., Heger, A., & Ferrara, A. 2005, *ApJ*, 633, 1031

Shiode, J. H., & Quataert, E. 2014, *ApJ*, 780, 96

Sukhbold, T., & Woosley, S. E. 2014, *ApJ*, 783, 10

Sukhbold, T., Ertl, T., Woosley, S. E., Brown, J. M., & Janka, H.-T. 2015, arXiv:1510.04643

Ugliano, M., Janka, H.-T., Marek, A., & Arcones, A. 2012, *ApJ*, 757, 69

Weaver, T. A., Zimmerman, G. B., & Woosley, S. E. 1978, *ApJ*, 225, 1021

Woosley, S. E., Heger, A., & Weaver, T. A. 2002, *Reviews of Modern Physics*, 74, 1015

Woosley, S. E., Blinnikov, S., & Heger, A. 2007, *Nature*, 450, 390

Woosley, S. E. 2010, *ApJ*, 719, L204

Woosley, S. E., & Heger, A. 2015, *ApJ*, 810, 34

Woosley, S. E., & Heger, A. 2015, *Very Massive Stars in the Local Universe*, 412, 199

Yoshida, T., Umeda, H., Maeda, K., & Ishii, T. 2016, *MNRAS*, 457, 351